Journal of Pharmaceutical and Biomedical Analysis 92 (2014) 90–97

Contents lists available at ScienceDirect

Journal of Pharmaceutical and Biomedical Analysis

journal homepage: www.elsevier.com/locate/jpba

A dynamic thermal ATR-FTIR/chemometric approach to the analysis of polymorphic interconversions. Cimetidine as a model drug

Natalia L. Calvo, Rubén M. Maggio, Teodoro S. Kaufman*

Area Análisis de Medicamentos, Departamento Química Orgánica, Facultad de Ciencias Bioquímicas y Farmacéuticas, Universidad Nacional de Rosario and Instituto de Química Rosario (IQUIR, CONICET-UNR), Suipacha 531, Rosario S2002LRK, Argentina

ARTICLE INFO

Article history:
Received 18 October 2013
Received in revised form
21 December 2013
Accepted 27 December 2013
Available online 7 January 2014

Keywords:
Crystal polymorphism
Multivariate curve resolution with alternating least squares (MCR-ALS)
Cimetidine
ATR-FTIR/chemometrics
Crystal form interconversion

ABSTRACT

Crystal polymorphism of active ingredients is relevant to the pharmaceutical industry, since polymorphic changes taking place during manufacture or storage of pharmaceutical formulations can affect critical properties of the products. Cimetidine (CIM) has several relevant solid state forms, including four polymorphs (A, B, C and D), an amorphous form (AM) and a monohydrate (M1). Dehydration of M1 has been reported to yield mixtures of polymorphs A, B and C or just a single form.

Standards of the solid forms of CIM were prepared and unequivocally characterized by FTIR spectroscopy, digital microscopy, differential scanning calorimetry and solid state ^{13}C NMR spectroscopy. Multivariate curve resolution with alternating least squares (MCR-ALS) was coupled to variable temperature attenuated total reflectance Fourier transform infrared spectroscopy (ATR-FTIR) to dynamically characterize the behavior of form M1 of CIM over a temperature range from ambient to 160 °C, without sample pretreatment.

MCR-ALS analysis of ATR-FTIR spectra obtained from the tested solid under variable temperature conditions unveiled the pure spectra of the species involved in the polymorphic transitions. This allowed the simultaneous observation of thermochemical and thermophysical events associated to the changes involved in the solid forms, enabling their unequivocal identification and improving the understanding of their thermal behavior.

It was demonstrated that under the experimental conditions, dehydration of M1 initially results in the formation of polymorph B; after melting and upon cooling, the latter yields an amorphous solid (AM). It was concluded that the ATR-FTIR/MCR association is a promising and useful technique for monitoring solid-state phase transformations.

1. Introduction

The quality of pharmaceutical products is currently assured on the basis of a scientific understanding of their physical and chemical properties that represent quality attributes. Crystal polymorphism is a property of the solid state by which a compound exhibits different solid crystalline phases, resulting from at least two different molecular arrangements. In Pharmaceutics, the term polymorphism is often employed to cover a variety of solids, including crystalline, amorphous, and solvate/hydrate forms. In that sense, amorphous forms are special cases of polymorphs, characterized by the absence of a regular crystal structure; additionally, solvates are often termed pseudo-polymorphs [1].

The polymorphs display different mechanical and physical properties, including crystal habit, lattice energy, intermolecular interactions, particle density, thermodynamic activity, melting point, solubility, stability, and dissolution rate [2]. These differences may have impact on the production process, changing manufacturing reproducibility and product performance, affecting drug dissolution, absorption and bioavailability [3].

The rational control of polymorphs of active pharmaceutical ingredients has been an important goal for the pharmaceutical industry; hence, proper characterization of the polymorphs is needed in order to gain better understanding of the physicochemical characteristics of the bulk drugs, which may influence their processability and capability to withstand the manufacturing processes and their stability during the storage period [4–6]. The inability to fully characterize drug polymorphic forms has led in the past to a number of problems, including the case of the protease inhibitor ritonavir, where formation of a previously unknown polymorph during the manufacturing stage led to a significant delay in the supplies of the capsule form [7].

Since polymorphs have different lattice energies, the less stable and more energetic species tend to convert to the most stable, less

* Corresponding author. Tel.: +54 341 4370477x118; fax: +54 341 4370477x112.
E-mail address: kaufman@iquir-conicet.gov.ar (T.S. Kaufman).

0731-7085/$ – see front matter © 2014 Elsevier B.V. All rights reserved.
http://dx.doi.org/10.1016/j.jpba.2013.12.036

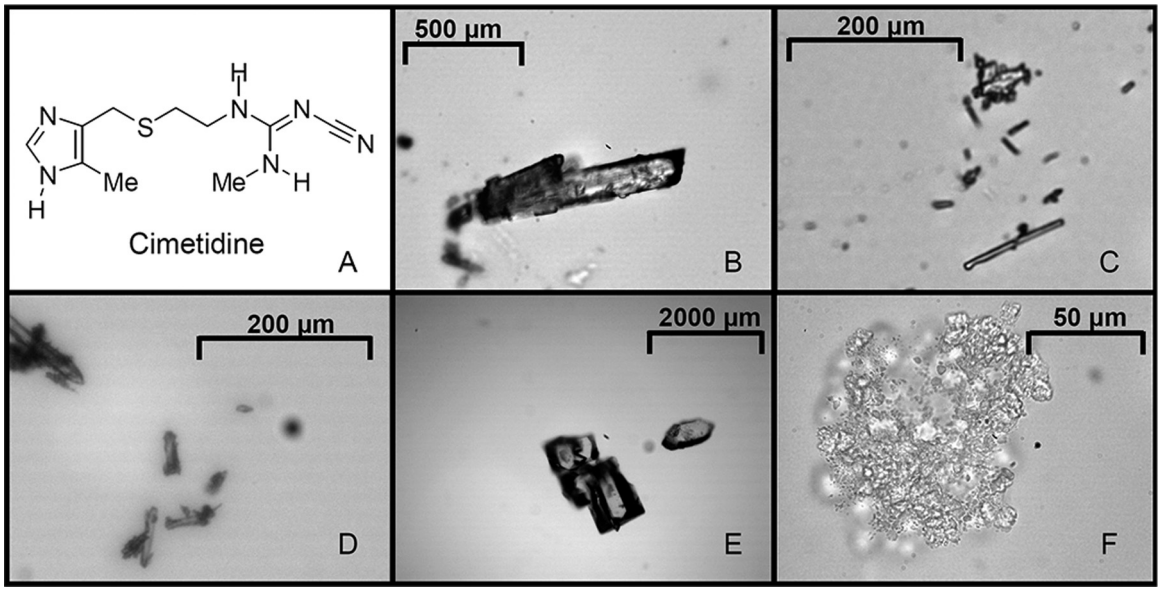

Fig. 1. (A) Chemical structure of Cimetidine. Optical microscopy of the polymorphs of cimetidine. (B) Form A. (C) Form B. (D) Form C. (E) Form D. (F) Form M1.

energetic, and likely the less soluble, crystal form. These transformations can take place during manufacturing operations (grinding, kneading and tableting); however, storage variables (temperature and humidity) may affect the stability of metastable crystal forms, and pharmaceutical excipients can also contribute to polymorphic conversions [8].

Cimetidine (CIM), one of the first blockbuster drugs, is (*Z*)-*N*″-cyano-*N*-methyl-*N*′[2-[[(5-methyl-1*H*-imidazol-4-yl)methyl]thio]ethyl]guanidine (Fig. 1A). The drug is a specific competitive antagonist of the histamine H2-receptor at the parietal cells [9], which inhibits the histamine-stimulated secretion of gastric acid and reduces pepsin output. Hence, CIM has been widely used in conditions where inhibition of gastric acid secretion may be beneficial, such as heartburn associated with acid reflux, duodenal and gastric ulcers, gastroesophageal reflux disease, and hypersecretory syndromes such as the Zollinger–Ellison's [10]. In addition, the drug is currently being considered for alternative indications [11].

Cimetidine has been discussed in the literature as a relevant example of a polymorphic substance, when crystallized under various conditions [12]. Four crystal modifications (A, B, C, D) and monohydrate M1 [13] have been described and characterized or differentiated by various methods, including infrared (IR), near infrared and Raman spectroscopy [14–17], X-ray diffraction [12,18,19], synchrotron X-ray powder diffraction [20], atomic force microscopy [21], solution calorimetry [22] and isotopic labeling-solid state NMR spectroscopy [23,24].

Polymorphic interconversions of CIM have also been recorded with isothermal calorimetry [25], and scanning thermal microscopy coupled to localized thermal analysis allowed to distinguish each of two forms [26], while differential scanning calorimetry (DSC) proved to have difficulties in identifying the different cimetidine polymorphs owing to the similarity in their bulk thermal behavior [27]. The thermodynamic stabilities of the anhydrous forms are extremely close to each other, in terms of heat of fusion, being hardly distinguished experimentally, so they have been considered 'practically isoenergetic' [27,28].

A number of additional pseudo-polymorphs [14,26,29,30] have been described, but their access could not be easily repeated. In addition, preparation of a fifth modification was reported, but the procedure could not be reproduced even by high-throughput crystallization experiments [31].

Interestingly, only three polymorphs were detected in a solvent screen including over 100 different conditions [32], while some published powder diffractograms still cannot be clearly attributed to specific crystal modifications [19]. The polymorphs differ in their bioavailability properties, principally due to their differences in dissolution rates [33–35]; however, in pharmaceutical formulations only modifications A and B are used [26]. Forms A, C, D and M1 have been resolved by X-ray crystallography [18,36–38]. It has been shown that even slight changes in crystallization or processing conditions (grinding, milling, etc.), sometimes not noticeable, are able to produce different crystal forms or their mixtures in an unpredictable manner [27]. In some cases, the obtained structures are identical; however their crystal parameters of the unit cell are somewhat different [16]. The presence of polymorphic mixtures in the commercial CIM product has been reported [38].

On the other side, it has been informed that, upon dehydration, the monohydrate M1 can be transformed into form A [19,24], or into forms A, B and C or a mixture of them, in an irreproducible manner, or to the modification already enclosed as an impurity [27].

Vibrational spectroscopy is a green tool for multicomponent analysis [39], which has proven to be suitable for measuring powder or polycrystalline samples for which even subtle changes in molecular structure need to be detected. Interestingly, however, in some cases FTIR analysis alone was unable to ascertain the composition of polymorphic forms of CIM [38].

Chemometric strategies are playing an increasingly important role in the analysis of multi-component mixtures and in the understanding of the most diverse phenomena. Several multivariate exploratory and resolution methods can be applied to the analysis of evolving mixtures, to provide information about pure compounds and their abundance in a sample; among them, the multivariate curve resolution with alternating least squares (MCR-ALS) approach is gaining wide acceptance due to its versatility [40].

The empowering of vibrational spectroscopies by association with MCR-ALS for the extraction of valuable information from complex evolving data has demonstrated to be highly successful [41,42]. Therefore, herein we report how a dynamic thermal attenuated total reflectance-FTIR/chemometrics strategy, with MCR as the chemometric tool (ATR-FTIR/MCR), may be used for monitoring the polymorphic transformation of a solid form, distinguishing

and characterizing the involved polymorphs. This potential is demonstrated for CIM, especially for the transformation of its monohydrate M1.

2. Materials and methods

2.1. Instrumentation

FTIR spectra were acquired in a Shimadzu Prestige 21 spectrometer (Shimadzu Corp., Kyoto, Japan) over a wavenumber range of 4000–600 cm^{-1}. ATR experiments were carried out with a diamond-based ATR accessory (GladiATR, Pike Technologies, Madison, USA) fitted with a Pike temperature control unit.

Calorimetric determinations were performed in a Shimadzu model 60 differential scanning calorimeter (Shimadzu Corp., Kyoto, Japan), operating under a constant flow of nitrogen (30 ml min^{-1}). The sample powders (10 mg) were placed in closed aluminum pans perforated with a pin-hole to equilibrate pressure from potential expansion of evolved gases or residual solvents, and heated at a rate of 5 °C/min between 40 and 160 °C. An empty pan was used as a reference.

Melting points were determined with an Electrothermal, model 9100 digital melting point instrument (Bibby Scientific Ltd., Staffordshire, UK). The samples were heated at 10 °C/min up to 10 °C below the temperature of interest; then, the heating rate was changed to 1 °C/min. In the case of M1, the heating rate was 1 °C/min.

Digital optical microscopy of the crystal forms was carried out with the aid of a Correct microscope (Seiwa Optical, Tokyo, Japan), fitted with 10×, 30× and 100× objectives and a 5.0 Megapixels Beion CMOS digital camera [Shanghai Beion Medical Technology Co., Ltd., Shangai, China; resolution 2592 × 1944 ($H \times V$)].

The high-resolution cross polarization-magic angle spinning (CP-MAS) ^{13}C solid state NMR spectra for polymorphs B and C were recorded using the ramp $\{^1H\} \rightarrow \{^{13}C\}$ CP-MAS sequence with proton decoupling during acquisition. All the solid-state NMR experiments were performed at room temperature in a Bruker Avance II-300 spectrometer equipped with a 4 mm MAS probe. The operating frequency for protons and carbons was 300.13 and 75.46 MHz, respectively. Glycine was used as an external reference for the ^{13}C spectra and to set the Hartmann–Hahn matching condition in the cross-polarization experiments. The recycling time was 15 s for sample B2 and 20 s for sample C2. Contact time during CP was 2 ms. The SPINAL64 sequence was used for heteronuclear decoupling during acquisition with a proton field H_{1H} satisfying $\omega_{1H}/2\pi = \gamma_H H_{1H} = 62$ kHz. The spinning rate for all the samples was 10 kHz.

2.2. Chemicals

The cimetidine bulk drug employed (polymorph A) was of pharmaceutical grade (BP 2002) and was acquired to Saporiti (Buenos Aires, Argentina). During the experiments, the drug was kept in a desiccator, protected from light. Double-distilled water was used for the preparation of aqueous solutions. All other chemicals were of analytical grade.

2.3. Preparation of the polymorphs of cimetidine

The forms A, B, C and D and M1 (monohydrate) were obtained by crystallization, as follows [14]. Form A was obtained after slowly cooling a hot (60 °C) saturated solution of the drug in isopropanol. Form B was obtained after cooling slowly a hot (70 °C) 15% aqueous solution of the drug. Form C was prepared by rapidly cooling to 5 °C a 5% aqueous solution of the drug. Form D was obtained by precipitation from a saturated solution of CIM in methanol/water (1:1, *v/v*) adjusted to pH 6 with acetic acid, which after being maintained at 25 °C, was brought to pH 8.5 in an ice bath by addition of concentrated ammonia. The M1 monohydrate was prepared by pouring a hot 15% aqueous solution over three times the amount of ice, prepared from distilled water [12,27,43]. The solids were filtered under reduced pressure, and the residue was stripped off of the remaining solvent under vacuum. The thus prepared solid forms were stored at room temperature, in dark screw-cap glass bottles. The amorphous form AM was obtained as a stable glassy solid by melting commercial polymorph A, followed by cooling down the liquid to room temperature [25]. For the experiments, the particle size of the samples was standardized by passage through a 50 mesh sieve.

2.4. FTIR determinations

Polymorph characterization was performed with the samples prepared as mulls suspended in Fluorolube® or with the pure solids, by the ATR technique. For polymorph conversion experiments, the spectrometer was coupled to the ATR accessory. Data acquisition was performed under predefined temperature conditions on 20 mg samples, at a resolution of 4 cm^{-1}, employing 20 scans per spectrum. Spectra were saved in .txt format for their further processing and analysis.

2.5. Chemometrics and graphics software

The computing routines involving spectral data manipulation and the MCR-ALS method were run in Matlab R2010a (Mathworks, Natick, USA). Full spectra (4000–600 cm^{-1}) were used without further processing. Statistical data analyses were performed with Origin 7.5 (OriginLab Co., Northampton, USA).

3. Theoretical background

The bases of MCR-ALS have been discussed in detail elsewhere [44,45]. A short theoretical background is given here. Boldface capital letters are used for matrices, and lowercase italics are used for scalars. The superscript "T" is employed to denote a transposed matrix, and $||\mathbf{X}||$ represents the norm of matrix **X**.

Assuming that the spectroscopic data fit an additive linear model conforming to Beer's law, the set of m spectra corresponding to mixtures containing contributions from k components acquired at n different wavenumbers, can be accommodated in a $m \times n$ experimental data matrix (**X**). In this way, the rows of **X** represent the spectra acquired in a time sequence, and each element x_{ij} in **X** is the absorbance of the ith sample, at the jth wavelength. MCR can be used to perform the optimal decomposition of **X** into the product of two smaller matrices, **C** and $\mathbf{S}^T$, as described in Eq. (1),

$$\mathbf{X}_{(m\times n)} = \mathbf{C}_{(m\times k)}\mathbf{S}_{(n\times k)}{}^{T} + \mathbf{E}_{(m\times n)} \quad (1)$$

where **C** is the matrix of the concentration profiles of the pure components and **S** is the matrix of their pure spectra. **E** is the residual matrix, which contains the information not explained by the model.

The above decomposition is performed employing a strategy which involves ALS. However, as a consequence of rotational or intensity ambiguity, the resulting solution is not unique, as more than one set of matrices **C** and **S** can reconstruct **X** by multiplication [46]. Restriction of the number of possible solutions to those embodied with physical meaning can be achieved by imposing constraints.

In addition, MCR-ALS requires initial estimates of **C** and **S**, which will be used to find a model able to minimize an error criterion, such as the lack of fit (*lof*) of the MCR data (x^*_{ij}) to the experimental values (x_{ij}), as detailed in Eq. (2). Previous knowledge of the system, such

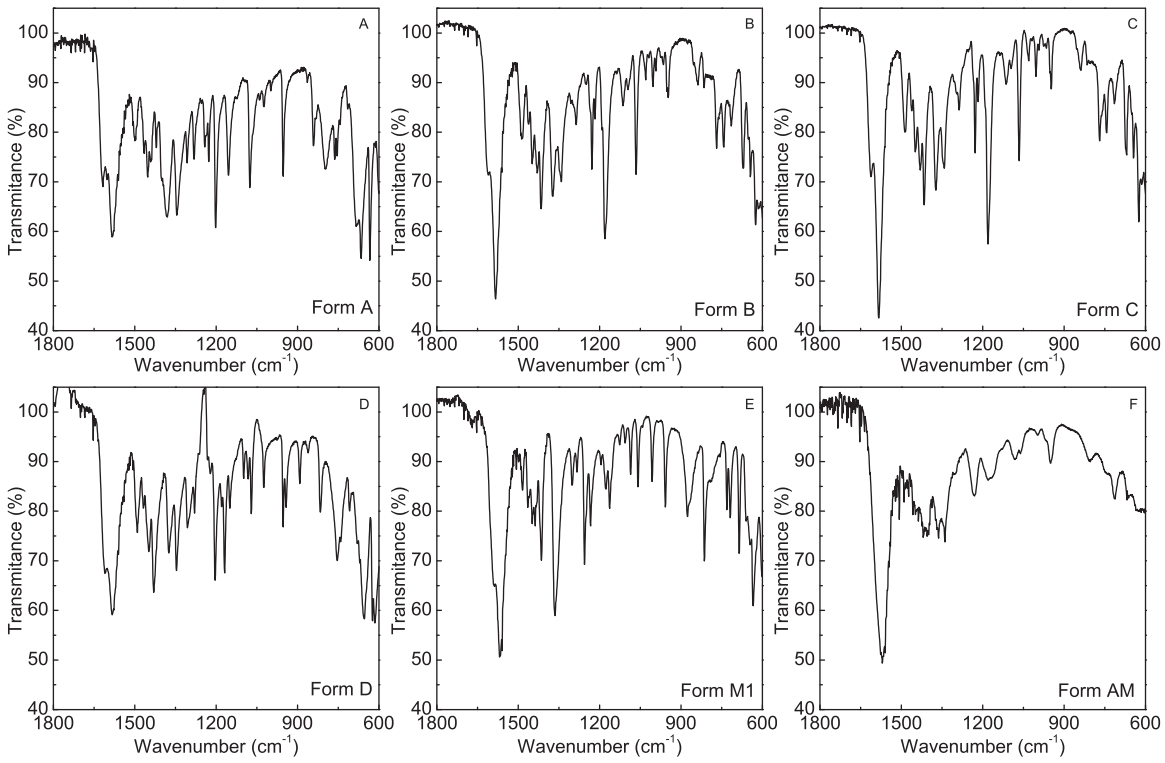

Fig. 2. ATR-FTIR spectra of different forms of CIM in the 1800–600 cm^{-1} region. Polymorphs A (A), B (B), C (C) and D (D); monohydrate M1 (E) and amorphous AM (F).

as the number of species involved and their corresponding spectra, can be employed to input initial guesses of **C** and **S** and add suitable constraints.

$$lof(\%) = 100 * \left(\frac{\sum_i \sum_j (x_{ij} - x_{ij}^*)^2}{\sum_i \sum_j x_{ij}^2} \right)^{0.5} \quad (2)$$

Given the initial estimates of **C** and **S**, matrix **X** is decomposed by iteratively solving two alternating least squares problems, the minimization of the error over **C** for fixed **S** and the minimization of error over **S** for fixed **C**. The cycle of iterations ends when the model error reaches a pre-established minimum value, according to Eqs. (3) and (4).

$$\text{Min}(\mathbf{C}) \| \mathbf{X} - \mathbf{C}\mathbf{S}^T \| \rightarrow \mathbf{C} = \mathbf{X}\mathbf{S}(\mathbf{S}^T\mathbf{S}) \quad (3)$$

$$\text{Min}(\mathbf{S}^T) \| \mathbf{X} - \mathbf{C}\mathbf{S}^T \| \rightarrow \mathbf{S} = \mathbf{X}^T\mathbf{C}(\mathbf{C}^T\mathbf{C}) \quad (4)$$

Statistical comparison of the MCR-derived spectra for each species with the spectra of the corresponding reference standards employing Pearson's correlation coefficient (r) can be used as an indicator to assess the quality of the results.

4. Results and discussion

4.1. Characterization of the solid forms

Polymorphs A, B, C, D and monohydrate M1 were obtained. Since inconsistent nomenclature of the polymorphic forms has been used throughout the literature by different authors [14,16,22,31], the modifications were unequivocally characterized by digital optical microscopy, ATR-FTIR spectroscopy, DSC and CP-MAS ^{13}C NMR solid state spectroscopy. Designation of the polymorphs is according to Hegedüs and Görög [14].

Digital optical microscopy revealed the crystalline habits of the polymorphs (Fig. 1). Form A was distinguished as platelets, polymorph B appeared as fine sharp needles, form C was observed as short needles, while polymorph D presented prismatic crystals, and M1 was seen as aggregated particles, in full agreement with the literature, where scanning electron microscopy revealed them to consist of small pyramidal crystals [19,25].

For ATR-FTIR characterization, the temperature (30 °C), particle size, amount of sample and the pressure exerted on the sample during the measurement were standardized. Under these conditions (Fig. 2), polymorphs B and C exhibited highly similar spectra. This similarity has led other researchers to suppose that they were the same substance [15,27]. Taking into account previous reports indicating that modification C is hardly reproducible [14] and readily transformed into form B upon minor mechanical treatment, such as trituration by hand in an agate mortar [27], in order to ensure its integrity extreme precautions regarding these factors were taken when polymorph C was handled.

Furthermore, in order to unequivocally ensure their identities, forms B and C were characterized by CP-MAS ^{13}C NMR solid state spectroscopy (Fig. 3), resulting in full agreement with those reported by the group of Middleton [23].

In the DSC analysis, the anhydrous forms A, B and D exhibited single peaks (Fig. 4A), without shoulders, at 145.0, 147.1 and 147.8 °C, respectively, corresponding to their melting points.These were in good agreement with data recorded with the melting point apparatus, where all melted samples solidified to yield a glassy amorphous solid. On the other hand, the monohydrate form M1 (Fig. 4B) exhibited an endothermic transition beginning at 58.55 °C with a peak at 72.30 °C, followed by a small exothermal curve at 81.05 °C. This was interpreted as a result of the loss of water accompanying the transition from M1 to an anhydrous form. A second endotherm, at 142.86 °C, corresponds to the melting point of the anhydrous form. Both endothermic transition temperatures were in agreement with those recorded by the melting point apparatus. The calculated heat of transition was 140.12 mJ mg^{-1}, in good agreement with the literature (140.5 mJ mg^{-1}) [27]. Table 1 summarizes the most relevant characteristic data of the different forms.

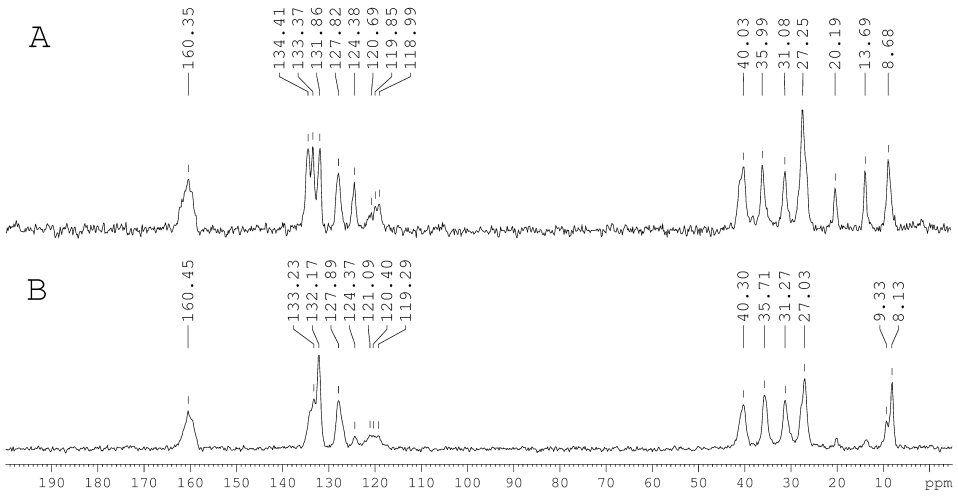

Fig. 3. Proton-decoupled CP-MAS ^{13}C NMR spectra (at 75.46 MHz) of polymorphs C (A) and B (B) of CIM.

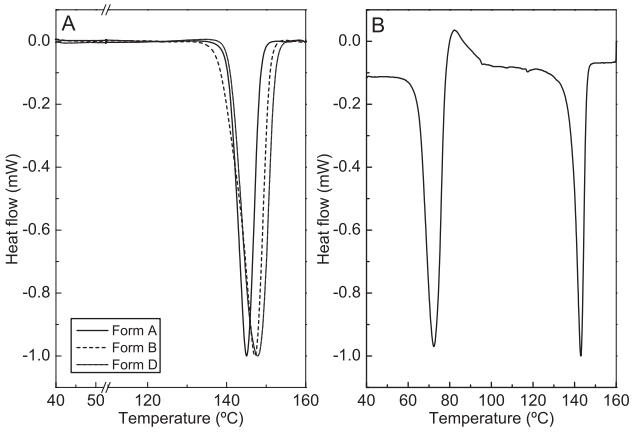

Fig. 4. DSC behavior of CIM. (A) Forms A, B and D. (B) Monohydrate M1.

4.2. Dynamic thermal ATR-FTIR/chemometrics monitoring of the conversion of M1

The first step in MCR analysis of the spectral data matrix is to determine its chemical rank, i.e., the number of absorbing species or contributing components. Principal component analysis (PCA) is one of the most widely used approaches to estimate the chemical rank of a series of spectral data.

PCA of the matrix containing the acquired ATR-FTIR data resulting from monitoring the effect of heating on M1 and inspection of the resulting screen plot [47] revealed the presence of three different forms (Fig. 5). Therefore, the computation was initialized with three components, including the spectra of the solid forms M1 and AM. A random vector, which was input to initialize the third component in order to avoid prediction bias.

MCR constraints, such as non-negativity of spectral concentrations and intensities, were also applied in order to confer physical sense to the results. The closure restriction of concentration values (sum of the abundances of the analytes' established as 1) was also

Table 1
Summary of physical properties of the different forms of CIM.

	Form A	Form B	Form C	Form D	Monohydrate M1
DSC (°C) [ET = endotherm]	144.99	147.09	143.44[a]	147.81	Onset ET1: 58.55 ET1: 72.30 ET2: 142.86 H_{trans} = 140.12 mJ mg^{-1}
Melting point (°C)	140.3	142.0	141.9	141.9	69.1 and 141.3
Crystal morphology (optical microscopy)	Thin platelet	Fine needle	Needle	Prism	Pyramid
FTIR, characteristic bands (ν_{max}, cm^{-1})	3208	3224	3230	3281	3497
	3142	3148	3152	3201	3384
	2923	2941	2943	2906	3298
	2171	2163	2162	2151	2151
	1615	1606	1606	1605	1591
	1579	1582	1581	1579	1449
	1451	1415	1413	1489	1414
	1377	1370	1370	1372	1256
	1201	1227	1227	1306	1163
	1153	1189	1178	1205	1006
	1074	1180	1064	1070	958
	952	1174	946	952	814
	665	1064	767	754	634

[a] Open pan.

Table 2
Pearson's correlation coefficients (r) of the MCR pure spectra and the reference spectra of the solid forms of CIM, in different spectral regions.

Origin of the spectrum		Pearson's r values[a] in the spectral region (cm^{-1})		
MCR spectrum	Solid form	Full spectrum (4000–600)	Fingerprint zone (1650–600)	C—H/N—H stretching (3600–2500)
S1	M1[b]	0.985	0.976	0.979
S2	A	0.814	0.814	0.589
	B[b]	0.988	0.952	0.953
	C	0.934	0.897	0.949
	D	0.844	0.844	0.730
S3	M[b]	0.969	0.978	0.991
Number of datapoints (n)		3527	1090	1142

[a] Cut off value for the similarity test at this stage was arbitrarily set at $r = 0.950$.
[b] Best-matching species.

added, based on the fact that the no change in the number of moles of cimetidine takes place during the studied process.

MCR-ALS performed the spectral deconvolution of the experimental data matrix [48] uncovering the temperature-dependent evolution of the three species, and revealing that they coexisted only in pairs (Fig. 5B).

Statistical comparisons between the spectra of the authentic pure forms of CIM and those offered by MCR-ALS were carried out employing Pearson's correlation coefficients (r) between the corresponding spectral vectors. Correlations were performed in the whole spectral region (4000–600 cm^{-1}), as well as in the fingerprint zone (1650–600 cm^{-1}) and along the 3600–2500 cm^{-1} range, which contains the fundamental bands corresponding to C—H and N—H stretching of CIM [49].

As stemmed from the results consigned in Table 2, the spectral information recovered after the MCR-ALS deconvolution process was highly correlated with the spectra of the standards of some solids. Values exceeding 0.95 were considered satisfactory, ensuring selectivity of the time-composition profiles.

Polymorphs B and C exhibited the best correlations. When the full spectra of both pure compounds were compared with S2, r values of 0.988 and 0.934 were obtained for forms B and C respectively, demonstrating a better overall fit for polymorph B.

Infrared spectra of forms B and C are very similar; however, Hegedüs and Görög [14] found some bands and regions which show differential properties and can be employed as diagnostic tools to assign polymorphic identity. Therefore, in order to further ensure the correct assignment of the intermediate form S2 to either polymorph B or C, a similar but more thorough Pearson's r-based strategy was followed, as an additional step.

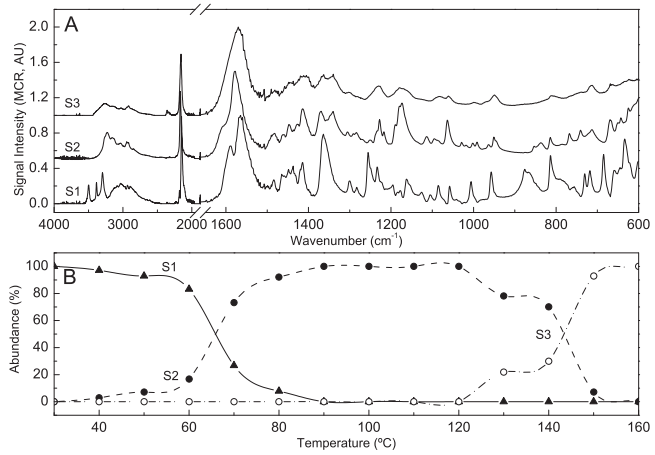

Fig. 5. Dynamic thermal ATR-FTIR/chemometrics monitoring of the heat-mediated transformation of the monohydrate M1 of CIM. (A) MCR-ALS output. Spectra of the species involved. (B) Concentration profiles of the different species during the process.

In this second instance, informative spectral ranges (Table 3) were examined, including the regions between 3400 and 2700 cm^{-1} (C—H/N—H stretching), 3009 and 2909 cm^{-1} (covering the peak at 2959 cm^{-1} [14]), 1750 and 1650 cm^{-1} (to include characteristic peaks of forms B and C), obtained by differential comparison between the pure FT-IR spectra), and that between 1243 and 1050 cm^{-1} (to include the characteristic peak at 1180 cm^{-1} [14]). In all cases, the r-values were higher for form B, demonstrating its better fit to the S2 spectrum provided by MCR. In addition, similar results were observed when the spectra were systematically divided into 200 cm^{-1} bins and compared pairwise.

These results confirmed that the crystal forms involved in the monitored transformation were the starting monohydrate M1 (Fig. 6A), which agreed with S1 ($r = 0.985$), and a second polymorph formed by dehydration of the monohydrate (Fig. 6B), which was identified as form B, taking into account the values of r between the spectrum of form B ($r = 0.988$) and the spectrum provided by MCR-ALS for S2.

On the other hand, this analysis confirmed that spectrum S3 (Fig. 6C) was in good statistical agreement with that of the amorphous melted form AM ($r = 0.969$), which began to form when polymorph B approached its melting point, and it was observed to solidify upon cooling to give a glassy solid. The lack of fit value between the MCR-ALS resolution results and the original **X** matrix was lower than 5%, ensuring the suitability of both, the output spectra and concentration profiles.

Interestingly, spectra of forms A, B, C and D exhibited characteristic peaks corresponding to the C≡N stretching band of the nitrile moiety at 2176 [43], 2171, 2164 and 2150 cm^{-1}, respectively, while S2 displayed a maximum at 2167 cm^{-1}.

Once the involved species were identified, the transitions among the different forms could be easily determined employing their time-concentration profiles. The transition temperatures obtained for the conversions M1 → B and B → AM were approximately 66.0 °C and 143.5 °C, being in good agreement with the observed DSC plots and with the literature.

The anhydrous forms (A, B, C and D) did not present thermally-induced interconversion into another polymorph before melting; however, all of them melted in the 140–150 °C range, furnishing a liquid which solidified to afford a glassy solid (AM), which did not crystallize.

Table 3
Pearson's r values for the comparison of forms B and C of CIM against S2 along key differential spectral regions.

Wavenumber range (cm^{-1})		Spectral information	Pearson's r coefficient	
Initial	Final		S2 vs. B	S2 vs. C
3400	2701	C—H/N—H stretching	0.978	0.923
3009	2909	Peak at 2959 cm^{-1} [14]	0.955	0.911
1750	1650	Diagnostic region	0.941	0.760
1243	1050	Peak at 1180 cm^{-1} [14]	0.923	0.877

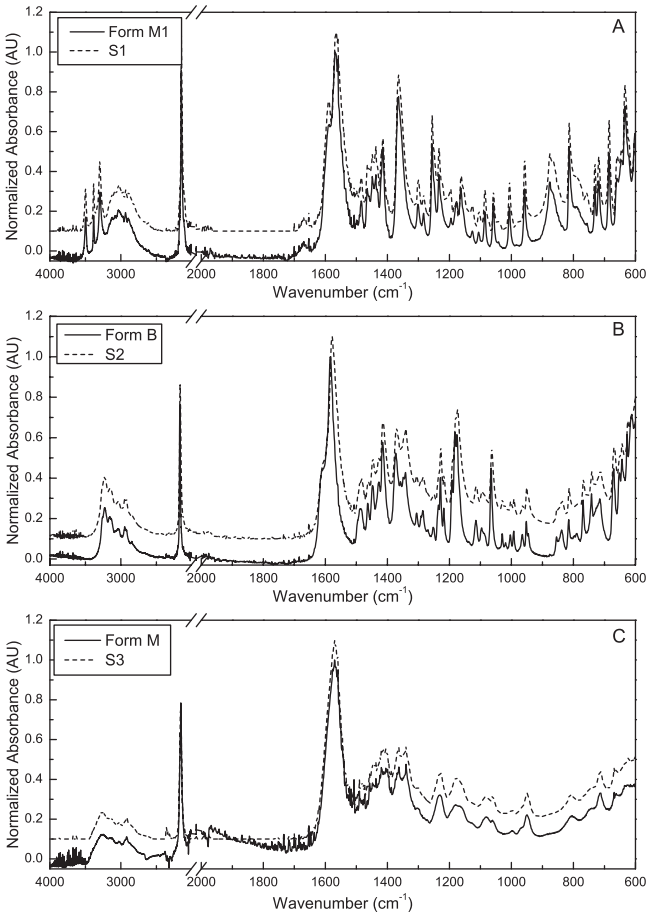

Fig. 6. Stacked graphics for comparison between the spectra of solids forms M1 (A), B (B) and AM (C), and those provided by MCR-ALS deconvolution S1 (A), S2 (B) and S3 (C), respectively.

5. Conclusions

Dynamic thermal ATR-FTIR spectroscopy coupled with MCR-ALS (ATR-FTIR/MCR), provided a valuable alternative for monitoring the polymorphic transformations of monohydrate M1 of cimetidine (CIM). Statistical comparison of the ATR-FTIR spectra of authentic solid forms of the drug with the spectra provided by MCR was able to reveal that upon heating, M1 dehydrates to yield polymorph B at approximately 66.5 °C, which agrees with the transition temperature previously informed in the literature. In turn, further increase in the system temperature leads to the conversion of form B into another species, with a melting point of approximately 143.5 °C, in accordance with literature data on the melting point of polymorph B. The monitoring system also revealed that the melted drug solidified upon cooling to yield a glassy amorphous solid (AM).

Thus, MCR-ALS analysis of the acquired series of spectra provided an accurate picture of the time evolution of the process, and this approach was also found to be useful in estimating the underlying spectra of the intervening forms, allowing to identify the species involved at all times, unlike the calorimetric techniques.

The method required only minor amounts of sample, since cumulative spectral acquisition followed by Fourier transform of the data compensated for low signal amplitudes. On the other hand, no sample preparation steps were involved. Therefore, the proposed approach should be considered as a useful strategy with high potential as a tool for gaining insight into the behavior of solid forms of active pharmaceutical ingredients, when they are subjected to thermal stress.

Acknowledgements

The authors are thankful to Secretaría de Ciencia Tecnología e Innovación (SECTeI), Consejo Nacional de Investigaciones Científicas y Tecnológicas (CONICET), Agencia Nacional de Promoción Científica y Tecnológica (ANPCyT), Secretaría de Ciencia y Tecnología de la UNR (SECyT-UNR) for financial support and Dr. Jorge Malarría (IFIR-CONICET) for facilitating access to the DSC equipment. NLC acknowledges CONICET for her fellowship.

References

[1] H.G. Brittain (Ed.), Polymorphism in Pharmaceutical Solids, 2nd ed., Informa Healthcare, Inc., NY, USA, 2009.
[2] J. Aaltonen, M. Allesø, S. Mirza, V. Koradia, K.C. Gordon, J. Rantanen, Solid form screening – a review, Eur. J. Pharm. Biopharm. 71 (2009) 23–37.
[3] D. Singhal, W. Curatolo, Drug polymorphism and dosage form design: a practical perspective, Adv. Drug Deliv. Rev. 56 (2004) 335–347.
[4] A. Llinás, J.M. Goodman, Polymorph control: past present and future, Drug Discov. Today 13 (2008) 198–210.
[5] D.E. Bugay, Characterization of the solid-state: spectroscopic techniques, Adv. Drug Deliv. Rev. 48 (2001) 43–65.
[6] A.W. Newman, S.R. Byrn, Solid-state analysis of the active pharmaceutical ingredient in drug products, Drug Discov. Today 8 (2003) 898–905.
[7] J. Bauer, S. Spanton, R. Henry, J. Quick, W. Dziki, W. Porter, J. Morris Ritonavir, An extraordinary example of conformational polymorphism, Pharm. Res. 18 (2001) 859–866.
[8] N. Chieng, T. Rades, J. Aaltonen, An overview of recent studies on the analysis of pharmaceutical polymorphs, J. Pharm. Biomed. Anal. 55 (2011) 618–644.
[9] N. Hall, A landmark in drug design, Chem. Brit. 33 (1997) 25–27.
[10] S.C. Sweetman (Ed.), Martindale: The complete Drug Reference, 35th ed., Pharmaceutical Press, London, UK, 2007.
[11] M. Kubecova, K. Kolostova, D. Pinterova, G. Kacprzak, V. Bobek Cimetidine, An anticancer drug? Eur. J. Pharm. Sci. 42 (2011) 439–444.
[12] B. Prodic-Kojic, F. Kajfes, B. Belin, R. Toso, V. Sunjic, Study of crystalline forms of *N*-cyano-*N*′-methyl-*N*-2-[[(4-methyl-1*H*-imidazol-5-yl)methyl]thio] guanidine (cimetidine), Gazz. Chim. Ital. 109 (1979) 535–539.
[13] K. Harsányi, G. Domány, L. Toldy, Cimetidine monohydrate and processes for its preparation and use, Patent GB 2101991, June 24, 1982.
[14] B. Hegedüs, S. Görög, The polymorphism of cimetidine, J. Pharm. Biol. Anal. 3 (1985) 303–313.
[15] A.M. Tudor, M.C. Davies, C.D. Melia, D.C. Lee, R.C. Mitchell, P.J. Hendera, S.J. Church, The application of near infrared FT-Raman spectroscopy to the analysis of the polymorphic forms of cimetidine, Spectrochim. Acta 47A (1991) 1389–1393.
[16] M. Baranskaa, L.M. Proniewicz, FT-IR and FT-Raman spectra of cimetidine and its metallocomplexes, J. Mol. Struct. 511–512 (1999) 153–162.
[17] G. Jalsovsky, O. Egyed, S. Holly, B. Hegedüs, Investigation of the morphological composition of cimetidine by FT Raman spectroscopy, Appl. Spectrosc. 49 (1995) 1142–1145.
[18] E. Hadicke, F. Frickel, A. Franke, Die Struktur von Cimetidin (*N*-Cyan-*N*-Methyl-*N*′-[2-[[(5-methyl-1*H*-imidazol-4-y1)methyl]thio]ethyl]guanidin), einem Histamin H2-Rezeptor-Antagonist, Chem. Ber. 111 (1978) 3222–3232.
[19] M. Shibata, H. Kokubo, K. Morimoto, K. Morisaka, T. Ishida, M. Inoue, X-ray structural studies and physicochemical properties of cimetidine polymorphism, J. Pharm. Sci. 72 (1983) 1436–1442.
[20] R.J. Cernik, A.K. Cheetham, C.K. Prout, D.J. Watkin, A.P. Wilkinson, B.T. Willis, The structure of cimetidine ($C_{10}H_{16}N_6S$) solved from synchrotron-radiation X-ray powder diffraction data, J. Appl. Cryst. 24 (1991) 222–226.
[21] A. Danesh, X. Chen, M.C. Davies, C.J. Roberts, G.H.W. Sanders, S.J.B. Tendler, P.M. Williams, M.J. Wilkins, Polymorphic discrimination using atomic force microscopy: distinguishing between two polymorphs of the drug cimetidine, Langmuir 16 (2000) 866–870.
[22] P.O. Souillac, P. Dave, J.H. Rytting, The use of solution calorimetry with micellar solvent systems for the detection of polymorphism, Int. J. Pharm. 231 (2002) 185–196.
[23] D.A. Middleton, C.S. Le Duff, F. Berst, D.G. Reid, A cross-polarization magic-angle spinning ^{13}C NMR characterization of the stable solid-state forms of cimetidine, J. Pharm. Sci. 86 (1997) 1400–1402.
[24] D.A. Middleton, C.S.L. Duff, X. Peng, D.G. Reid, D. Saunders, Molecular conformations of the polymorphic forms of cimetidine from ^{13}C solid-state NMR distance and angle measurements, J. Am. Chem. Soc. 122 (2000) 1161–1170.
[25] M. Otsuka, F. Kato, Y. Matsuda, Physicochemical stability of cimetidine amorphous forms estimated by isothermal microcalorimetry, AAPS PharmSciTech 3 (2002) 32–44.
[26] G.H.W. Sanders, C.J.R. Roberts, A. Danesh, A.J. Murray, D.M. Price, M.C. Davies, S.J.B. Tendler, M.J. Wilkins, Discrimination of polymorphic forms of a drug product by localised thermal analysis, J. Microsc. 198 (2000) 77–81.
[27] A. Bauer-Brandl, Polymorphic transitions of cimetidine during manufacture of solid dosage forms, Int. J. Pharm. 140 (1996) 195–206.
[28] A. Bauer-Brandl, E. Marti, A. Geoffroy, A. Poso, J. Suurkuusk, E. Wappzer, K.H. Bauer, Comparison of experimental methods and theoretical calculations on

crystal energies of 'isoenergetic' polymorphs of cimetidine, J. Therm. Anal. Calorim. 57 (1999) 7–22.
[29] J. Bernstein, Polymorphism in Molecular Crystals, 73, Clarendon Press, Oxford, UK, 2002, pp. 255.
[30] P. Bencsik, S. Görög, M. Hajnóczy, B. Hegedüs, A. Jeszenszky, M. Kapás, G. Kozma, L. Nagy, Z. Papné Sziklai, E. Török, F. Végh, L. Vereckei Novel cimetidine polymorph and process for preparing same. Patent WO 92/14713, September 1992.
[31] E. Dova, A. van Langevelde, B. McKay, R. Peschar, E. Blomsma, High-throughput polymorph screen of cimetidine and clarification of its nomenclature, Acta Cryst. A61 (2005) C337.
[32] P.J. Desrosiers, The potential of preform, Mod. Drug Discov. (2004) 40–43.
[33] H. Kamiya, K. Morimoto, K. Morisaka, Dissolution behavior and bioavailability of cimetidine–HCl (cimetidine monohydrochloride monohydrate), Int. J. Pharm. 26 (1985) 197–200.
[34] T. Funaki, S. Furata, N. Kaneniwa, Discontinuous absorption property of cimetidine, Int. J. Pharm. 31 (1986) 119–123.
[35] H. Kokubo, K. Morimoto, T. Ishida, M. Inoue, K. Morisaka, Bioavailability and inhibitory effect for stress ulcer of cimetidine polymorphs in rats, Int. J. Pharm. 35 (1987) 181–183.
[36] L. Párkányi, A. Kálmán, B. Hegedüs, K. Harsanyi, J. Kreidl, Structure of a novel and reproducible polymorph (Z) of the histamine H_2-receptor antagonist cimetidine, $C_{10}H_{16}N_6S$, Acta Cryst. C40 (1984) 676–679.
[37] H. Birkedal, A. Bauer-Brandl, P. Pattison, The surprising polymorph C of cimetidine: synchrotron radiation to the rescue, in: XIXth 19th European Crystallographic Meeting, August 25–31, Nancy, France, 2000.
[38] A. Arakcheeva, P. Pattison, A. Bauer-Brandl, H. Birkedal, G. Chapuis, Cimetidine $C_{10}H_{16}N_6S$, form C: crystal structure and modelling of polytypes using the superspace approach, J. Appl. Cryst. 46 (2013) 99–107.
[39] J. Moros, S. Garrigues, M. de la Guardia, Vibrational spectroscopy provides a green tool for multi-component analysis, Trends Anal. Chem. 29 (2010) 578–591.
[40] T. Rajalahti, O.M. Kvalheim, Multivariate data analysis in pharmaceutics: a tutorial review, Int. J. Pharm. 417 (2011) 280–290.
[41] K. Kwok, L.S. Taylor, Analysis of counterfeit Cialis® tablets using Raman microscopy and multivariate curve resolution, J. Pharm. Biomed. Anal. 66 (2012) 126–135.
[42] G.P. Sabin, V.A. Lozano, W.F.C. Rocha, W. Romão, R.S. Ortiz, R.J. Poppi, Characterization of sildenafil citrate tablets of different sources by near infrared chemical imaging and chemometric tools, J. Pharm. Biomed. Anal. 85 (2013) 207–212.
[43] V. Tantishaiyakul, S. Songkro, K. Suknuntha, P. Permkum, P. Pipatwarakul, Crystal structure transformations and dissolution studies of cimetidine–piroxicam coprecipitates and physical mixtures, AAPS PharmSciTech 10 (2009) 789–795.
[44] A. de Juan, R. Tauler, Multivariate curve resolution (MCR) from 2000: progress in concepts and applications, Crit. Rev. Anal. Chem. 36 (2006) 163–176.
[45] C. Ruckebusch, L. Blanchet, Multivariate curve resolution: a review of advanced and tailored applications and challenges, Anal. Chim. Acta 765 (2013) 28–36.
[46] R. Rajkó, Computation of the range (band boundaries) of feasible solutions and measure of the rotational ambiguity in self-modeling/multivariate curve resolution, Anal. Chim. Acta 645 (2009) 18–24.
[47] R.B. D'Agostino, H.K. Russell, Scree test, in: Encyclopedia of Biostatistics, Wiley, New York, 2005.
[48] J. Jaumot, R. Gargallo, A. de Juan, TaulerF R., A graphical user-friendly interface for MCR-ALS: a new tool for multivariate curve resolution in MATLAB, Chemometr. Intell. Lab. Syst. 76 (2005) 101–110.
[49] W.A. Bueno, E.G. Sobrinho, Hydrogen bonds in the cimetidine molecule, Spectrochim. Acta A 51 (1995) 287–292.